Technical Report No. 32-467

Theoretical and Practical Aspects of Solar Pressure Attitude Control for Interplanetary Spacecraft

James D. Acord

John C. Nicklas

jpl

JET PROPULSION LABORATORY
CALIFORNIA INSTITUTE OF TECHNOLOGY
PASADENA, CALIFORNIA

May 15, 1964
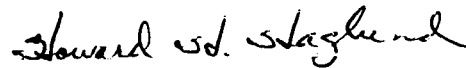
Technical Report No. 32-467

Theoretical and Practical Aspects of
Solar Pressure Attitude Control
for Interplanetary Spacecraft

James D. Acord

John C. Nicklas

H. H. Haglund, Chief
Guidance and Control Division

JET PROPULSION LABORATORY
CALIFORNIA INSTITUTE OF TECHNOLOGY
PASADENA, CALIFORNIA

May 15, 1964

CONTENTS

FIGURES

ABSTRACT

29002

This Report briefly covers the theory of photon momentum transfer to the exposed surfaces of a space vehicle, and gives an engineering derivation of the essential equations and parameters for dealing with the resulting forces in a practical manner. Various configurations of spacecraft equipment and control surfaces are examined as to magnitudes and directions of solar pressure torques and the necessary conditions for control. To illustrate the principles involved, a particular spacecraft configuration is chosen for further examination and analysis. Block diagrams and transfer functions are given for several control and damping-loop configurations.

Some of the major system-integration considerations are discussed, with particular emphasis on a minimum-interface combination of the solar pressure control system with an impulsive mass-expulsion system. System parameter optimization by graphical parametric analysis is illustrated, with the combined impulsive–solar-pressure system as an example.

Finally, some of the special considerations and peculiarities involved in mechanizing such a low-torque low-response control system are discussed. A practical, simple mechanization is presented to illustrate the salient points.

Author

I. INTRODUCTION

In the literature, there are many references to the effects of the solar photon pressure field on the attitude control and flight path of space vehicles (Refs. 1, 2, and 3). Although the forces are small, their neglect can cause trajectory errors of several thousand miles on a planetary mission and, if the spacecraft is improperly balanced, significant increases in attitude control gas consumption may result. On the basis of flight telemetry data from the *Mariner 2* Venus mission, it was determined that the spacecraft experienced solar pressure imbalance torques of at least 10 to 30 dyne-cm per axis. These torques alone accounted for about half of the total gas consumed.

In theory, it is relatively simple to design a passively stable spacecraft. It is necessary only to make certain that the centroid of solar pressure on the craft is "down Sun" from the center of mass (Refs. 4, 5, and 6). The action is analogous to that of a sea anchor that holds the bow of a boat into the wind during a storm. Unfortunately, such a configuration is not sufficient for control. In mechanizing a system utilizing a solar pressure control, the major problems fall into two areas:

1. Such a system has no inherent damping and would thus continuously oscillate about its neutral position with an amplitude depending on initial angular position and rate. Methods which have been proposed to obtain damping include some form of viscous friction working against a secondary inertia, or the use of a rate-feedback signal. While theoretically sound, the practical implementation of such systems at natural frequencies on the order of several hours per cycle (typical values) presents formidable problems.

2. The neutral position, or center of oscillation, of the passive system does not usually lie at the null position of the primary attitude control system. Prelaunch adjustment is manifestly unfeasible because of the extremely minute forces involved.

The method of solar pressure utilization discussed here presents a practical solution to these problems.

II. DERIVATION OF SOLAR PRESSURE FORCES

Consider a surface of area A whose normal vector is at an angle ψ radians to a collimated radiation field of power density I w/m², as shown in Fig. 1. Further assume that the surface reflects a fraction ρ (where $0 < \rho < 1$) of the incoming energy and absorbs a fraction $1-\rho$. Of the amount reflected, consider that a fraction s (where $0 < s < 1$) is reflected specularly, and a fraction $1-s$ is reflected diffusely or with uniform intensity, as seen from the hemisphere about the lighted side of the surface.

The incoming photons may be considered to have an equivalent mass in accordance with the famed electromagnetic mass–energy equivalence relationship $E = mc^2$. From this, the photon equivalent momentum P may be expressed as $P = E/c$. The force developed as a result of photon momentum transfer at a surface is entirely defined by the vector relationship $\mathbf{F} = d\mathbf{P}/dt$.

The area A intercepts a beam of radiation with cross section $A \cos \psi$. If that beam were entirely absorbed at the surface (i.e., $\rho = 0$), then the momentum transferred to the surface in unit time $d\mathbf{P}/dt$ is the total momentum of photons contained in a volume of cross section $A \cos \psi$ and length c. From the relation $P = E/c$, if P is now taken as P_v (the photon momentum in the volume of space $cA \cos \psi$), then E represents the photon energy in the same volume, or $E_v = IA \cos \psi$, the power density multiplied by the cross-sectional area. The power density I is the energy per unit time through unit area. Summing up for this case,

$$\left| \mathbf{F} \right| = \left| \frac{d}{dt} \mathbf{P} \right| = P_v = \frac{E_v}{c} = \frac{IA \cos \psi}{c}$$

The direction of the resulting force is the same as the direction of incoming radiation, since all photons are completely absorbed. A fundamental quantity to be used extensively in subsequent analysis may now be introduced:

$$P_f = \frac{I}{c}$$

where P_f is defined as the radiation pressure (force per unit area) acting on a nonreflective surface normal to the incoming radiation. Expressing P_f in convenient units,

$$P_f = 3.33 \times 10^{-4} I \tag{1}$$

Here, P_f is in dynes/m², and I is in w/m². Near Earth, $I = 1.4 \times 10^3$ w/m², and Eq. 1 yields $P_f = 0.47$ dynes/m².

As shown in Fig. 1, the momentum of the photons intercepted by the surface will be changed in various ways, depending on the surface conditions. From the foregoing discussion, if $\rho = 0$, the force developed on the surface would be $P_f A \cos \psi \, \mathbf{U}_I$, where $\mathbf{U}_I$ is a unit vector in the direction of incoming radiation. The components of radiation force $\mathbf{P}_a$, due only to absorbed photons, may then be calculated from the relation

$$\mathbf{F}_a = (1 - \rho) P_f A \cos \psi \, \mathbf{U}_I \tag{2}$$

Another force in this direction is due to proton flux. This force is generally small compared with that caused by the absorbed photons, but it may become significant during periods of increased solar activity. If it is desired to include this effect, it can be done by substituting an equivalent pressure P_e for the quantity $(1 - \rho) \, P_f$ in Eq. 2. In the remainder of this Report, it is assumed that the forces due to proton flux are negligible.

Of the fraction ρ of photons reflected from the surface, a subfraction $s\rho$ is reflected specularly as from a mirror, with the reflected beam and the incoming beam making equal angles with the normal to the surface. In this case, the normal component of momentum in the reflected ray is equal and opposite to that in the incoming ray for the $s\rho$ subfraction, and the tangential component is unchanged. Applying the law of momentum conservation at the surface, the component of force $\mathbf{F}_s$ due only to specularly reflected photons is given by

$$\mathbf{F}_s = 2s\rho \, P_f A \cos^2 \psi \, \mathbf{U}_n \qquad (3)$$

where $\mathbf{U}_n$ is a unit vector normal to the surface. The remaining subfraction $(1 - s)\rho$ of the reflected photons is assumed to be diffusely reflected. The incoming-photon momentum may be considered as stopped at the surface and subsequently reradiated uniformly into the hemisphere containing $-\mathbf{U}_n$. The force due to the stopping of the incoming photons $\mathbf{F}_{DI}$ may be calculated from Eq. 2 by changing the expression for the photon momentum subfraction from $1 - \rho$ to $(1 - s)\rho$:

$$\mathbf{F}_{DI} = (1 - s)\rho \, P_f A \cos \psi \, \mathbf{U}_I \qquad (4)$$

The outgoing momentum of diffusely reflected photons may be calculated by integrating over the hemisphere and making use of the symmetry about the normal to the surface. It is apparent that the tangential components of outgoing momentum will be cancelled, because symmetry leaves only the normal components to be integrated over the hemisphere. The result is that the effective momen-
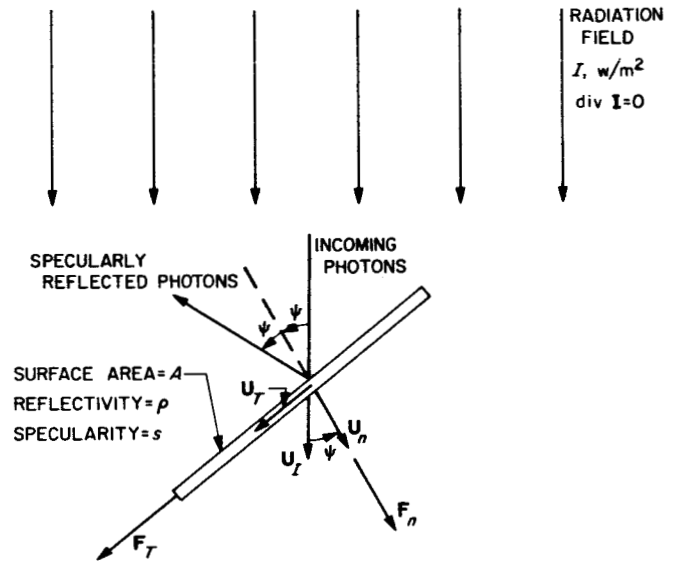
Fig. 1. Photons impinging on surface area

tum transfer to the surface due to outgoing diffusely reflected photons is just two-thirds of what it would have been had the same number of photons been reflected along the normal. The force $\mathbf{F}_{DR}$, due to diffuse reflection of the $(1 - s)\rho$ subfraction, is given by

$$\mathbf{F}_{DR} = (1 - s)\rho \, \frac{2P_f}{3} \, A \cos \psi \, \mathbf{U}_n \qquad (5)$$

Resolving the forces along the direction of incident radiation into normal and tangential components, and gathering terms, the total force vector $\mathbf{F}$ is

$$\mathbf{F} = \left[\frac{2\rho}{3}(1 - s) \cos \psi + (1 + s\rho) \cos^2 \psi \right] P_f A \, \mathbf{U}_n$$
$$+ (1 - s\rho) \, P_f A \cos \psi \sin \psi \, \mathbf{U}_T \qquad (6)$$

where $\mathbf{U}_T$ is a unit vector along the intersection of the surface with the plane containing $\mathbf{U}_I$ and $\mathbf{U}_n$, and is directed as shown in Fig. 1.

III. APPLICATION TO ATTITUDE CONTROL PROBLEM

In a system using forces generated by solar radiation pressure, special attention must be given to the static stability of the system and the manner in which damping can be introduced. A system is said to be statically stable

when the center of mass of the spacecraft lies between the Sun and the point of application of the resultant solar pressure force (Fig. 2). This point of application is called the center of pressure. In this case, whenever the

Fig. 2. Schematic of statically stable spacecraft

Fig. 3. Example of single-vane solar stabilizer

Fig. 4. Example of dual-vane solar stabilizer

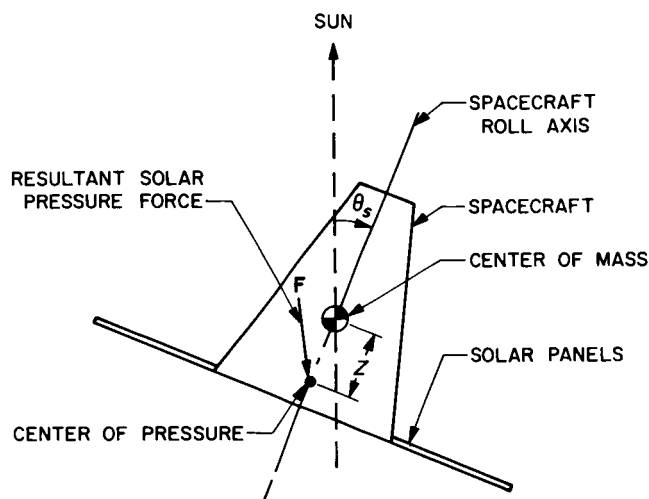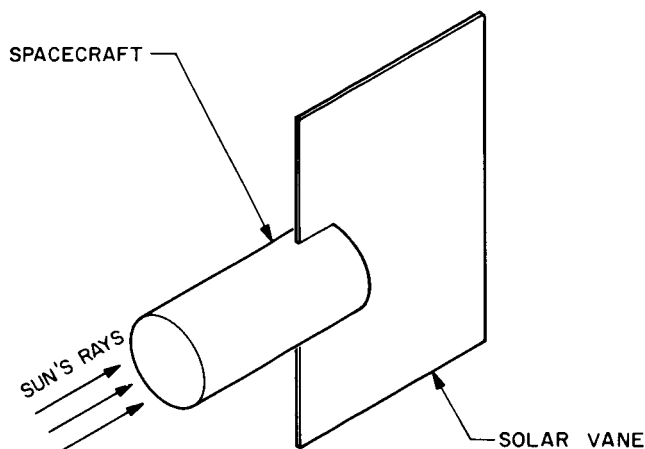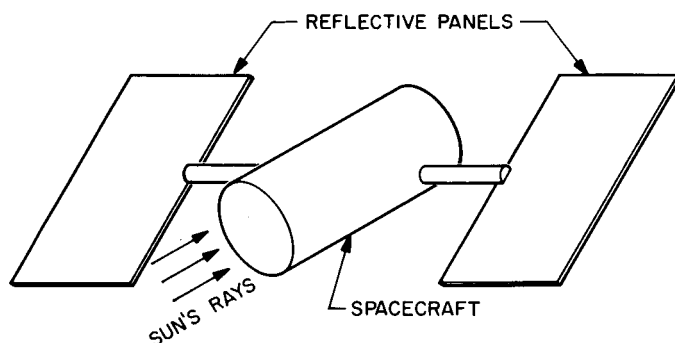tive panels have one or two degrees of freedom with respect to the spacecraft (Fig. 4). These panels are mounted in such a position that, with respect to the Sun, the resulting solar pressure force acts behind the center of mass of the spacecraft.

For a statically stable system, the stable position occurs when the center of pressure, the spacecraft center of mass, and the Sun are colinear. This is called the zero or null position of the spacecraft. Any rotating of the spacecraft about its center of mass is denoted by θ_s. If, for any reason, the spacecraft is disturbed from the null position, it will oscillate about this position with an amplitude depending upon the value of θ_s and $\dot{\theta}_s$ at the time that the disturbance disappears. For small angles, the equation of motion of the spacecraft is given by

$$J \ddot{\theta}_s + FZ\theta_s = 0 \qquad (7)$$

where

J = moment of inertia of the spacecraft about its center of mass

F = resultant solar pressure force

Z = distance between center of pressure and center of mass

Since Eq. 7 contains no damping term, any control system using solar pressure forces must be mechanized to include a means of damping.

Various techniques of obtaining damping have been suggested. In one method, a fluid is used to dissipate energy by means of viscous friction. Another proposed technique utilizes a rotor passing through a magnetic field to generate damping forces. More conventional means, such as the use of a rate-measuring device on the spacecraft and active control of the vane position, have been suggested. However, all these methods of obtaining damping have the same disadvantage: they would be very difficult to mechanize. In the technique proposed

spacecraft rotates away from the stable or null position, a restoring or stabilizing force occurs. However, if the center of pressure lies between the Sun and the center of mass, solar pressure will generate a destabilizing force whenever the spacecraft moves away from the null position. This is a statically unstable system.

There are several ways in which a system can be made statically stable. In one technique, a reflective vane-like appendage is used as a solar stabilizer. The vane is mounted to the spacecraft on the side away from the Sun so that, when the spacecraft has the proper attitude, the Sun's rays are parallel to the vane, and no forces are generated (Fig. 3). When the spacecraft and, hence, the vane are at some angle with respect to the Sun's rays, a restoring force will be developed tending to return the spacecraft to the null position. In another method, reflec-

Fig. 5. Undamped motion of statically stable spacecraft

is proportional to the negative of the velocity signal: i.e., to a signal leading θ by 90 deg and opposite to it in sign. This is termed *negative velocity feedback*. In a steady state condition for sinusoidal oscillations, this signal can also be described as lagging θ by 90 deg, and as being of the same sign. This is the same as the signal proportional to F_d described above.

If F_d lags θ by less than 90 deg, there are times when F_d is not a retarding force, but is causing the velocity to increase (Fig. 6). In this Figure, the shaded areas represent the impulse that would be expended in retarding the spacecraft, and the unshaded areas under the F_d curve show the impulse that would increase the velocity. As long as the shaded area exceeds the unshaded area, a net damping impulse remains, and the oscillations will decay to zero. It can be seen that some damping will be obtained whenever F_d lags θ by an angle greater than zero but less than 180 deg. Also apparent from this discussion is that the optimum case arises when the lag angle is 90 deg, as shown in Fig. 5. Thus, for a statically stable spacecraft, negative velocity feedback can be replaced by a positive feedback signal lagging the position.

A. System Integration

A glance at some typical parameters associated with practical spacecraft and control-surface dimensions demonstrates that, despite mathematical similarity, solar

here, this disadvantage is eliminated. It is necessary only that the spacecraft be statically stable. If this is the case, curves of position and velocity versus time are sinusoids, with the velocity leading the position by 90 deg, as shown in Fig. 5. The most effective damping occurs when a force is always in opposition to the velocity. This force F_d is shown as a sine wave in Fig. 5, and it lags θ by 90 deg. One is thus led to the conclusion that damping can be obtained by using a force which lags the position by 90 deg. As a substitute for this intuitive approach, the terms of servo analysis can be used to describe the damping requirements. In the usual system, the damping force
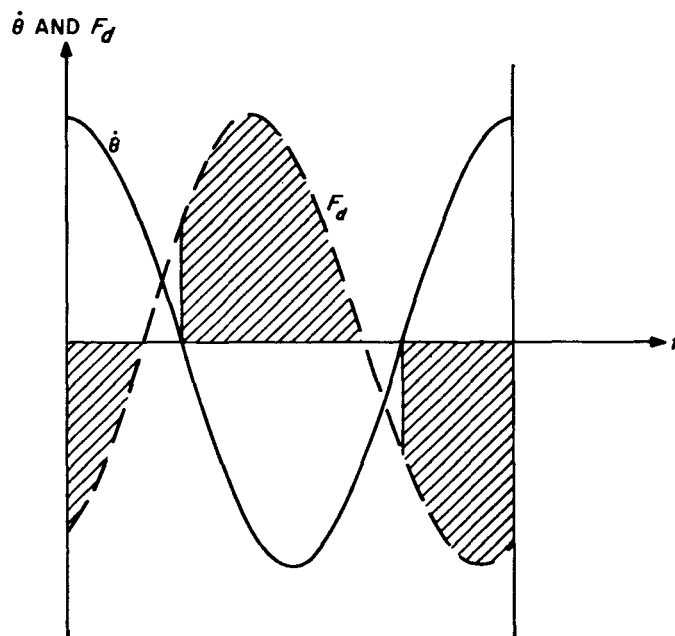

Fig. 6. Damping force on statically stable spacecraft

pressure control systems require an almost entirely new technology, which is discussed more fully in Section IV. The item of primary interest at this point is that the extremely low torques and slow response speeds of such systems make them useful mainly for long-term-cruise control on interplanetary flights. The more dynamic flight phases, such as initial attitude acquisition and attitude maneuvering, generally require faster-acting higher-torque systems, such as conservative momentum-interchange systems using torqued flywheels or gyros, or nonconservative systems using hot or cold gas jets. To illustrate the aspects of system integration involved, a conservative flywheel system is briefly considered, followed by a more detailed study involving an impulsive cold gas jet system (Ref. 7).

If a momentum-conservative primary attitude control system is used alone, the angular momentum of the total spacecraft must remain constant. Thus, during the initial stabilization process, any angular momentum removed from the body of the spacecraft must be stored on the flywheels. In addition, any external bias torques due to magnetic-field interaction, gravitational gradients, outgassing of equipment, or radiation-torque imbalances will result in continuous acceleration of the flywheels and eventual saturation or centrifugal destruction of these components. A set of solar pressure control surfaces, properly adjusted, can accomplish two important tasks in such a system with relatively simple control logic. The control surfaces should be continuously adjusted so that the resulting solar pressure torque about each spacecraft axis is proportional to some function of the flywheel velocity and its integral about that axis. If the intentional imbalance-torque so derived is in a direction to force reduction of the wheel velocity through the primary control system, a nearly ideal situation results. The accumulated wheel momentum is first slowly worked off against the intentional solar pressure imbalance. The imbalance is reduced as the wheel speed is reduced until a steady state condition is reached, with the wheel running at a low constant speed, and the control surfaces set to balance out all external torques. Such a cooperative system has many advantages. It requires no mode-switching, with the attendant reliability problems; it can be a linear system capable of very tight angular accuracy; and it uses high-power high-response control only when required by the control task.

In considering solar pressure control as a cooperative element with an impulsive cold gas attitude control system, it is convenient to start by defining the total system design goals and, from these, to develop the guidelines

for integration. Probably the most important system design goals are the following:

1. *Maximum mass efficiency.* This is the ratio between the total control angular impulse actually required by the spacecraft mission profile and the total system weight, including fuel, allocated to perform that control task. The ratio may be considered as the product of three sub-ratios: specific impulse of fuel; mass fraction of system, or ratio of fuel weight to total system weight; and control system design efficiency. The first two are generally familiar terms, and their product may be defined as a total system specific impulse. The third is calculated by first summing the angular impulse required to overcome all disturbances, intentional or otherwise, for the complete mission, and then dividing by the linear impulse actually carried to perform the total task. If the gas jet system is used alone, its design efficiency may be improved by such measures as:

   a. Increasing the jet lever arm to increase the ratio of angular impulse to linear impulse.

   b. Reducing the turning rates during attitude reorientations to minimize the acceleration and deceleration time.

   c. Increasing the limit cycle size and decreasing the limit cycle velocity. These changes have an effect only if the spacecraft is torque-balanced precisely enough that an actual limit cycle occurs (Ref. 7). Experience has shown this to be virtually impossible without some means of adjusting the center of mass or the center of radiation pressure, or both, in flight.

   d. Reducing contingency reserves.

   Obviously, the ideal system would not require any expenditure of impulse to maintain either a fixed position or a constant velocity with respect to the inertial reference frame.

2. *Minimum electrical peak power and total energy.* Electrical power requirements for attitude control may be divided into two parts. The first is a preferably small constant demand to operate sensors and standby signal-processing electronic circuitry. This is minimized by the usual circuit design techniques. The second is the incremental power required when the jet valves or other intermittent loads are actuated. The peak power levels of these loads are of concern, as well as their duty cycle or total duration, which is related to the design efficiency defined above.

3. *Maximum reliability.* Reliability may be defined in many ways, but the definition best suited to the present discussion is *performance of the attitude control task for the total mission.* In addition to its dependence on the usual items (component types, counts, load factors, and equipment operating time), the reliability of an attitude control system is critically dependent on the number of actuations of intermittently operating components, such as gas valves, relays, etc.

The task of system integration is to define the interfaces between the primary gas jet system and the cooperating, but secondary, solar pressure system so as to maximize the degree of design-goal achievement. The solar pressure system must be regarded as secondary, because it cannot perform the total attitude control task alone, whereas the gas jet system can. A properly integrated solar pressure system can significantly contribute to design goals (1) and (3) above, while causing little or no degradation of goal (2). On the basis of these considerations, the following system-interface guidelines are listed:

1. The number and complexity of electrical interfaces between the primary control system and the solar pressure system should be reduced to an absolute minimum and should be designed to favor the reliability of the primary system.

2. The most important duty of the solar pressure control system should be to balance out all external torques on the spacecraft. Minimum external torque results in near-minimum gas consumption and a greatly reduced number of jet actuation cycles, thus contributing to all three design goals.

3. The two control systems should be cooperative, not exclusive, in their operation. Otherwise, one system would have to be shut down during operation of the other to avoid "fighting." This implies that the null or balance point of the solar pressure system must be adjustable to fall within the jet system dead band.

The overall system proposed in this Report is now examined with special reference to the guidelines listed above. The system is based on primary control by a minimum-impulse cold nitrogen gas jet system (Ref. 7) similar to that used on *Mariner 2.* To the basic system is added an array of four solar pressure control surfaces with their actuators and control electronics. Both the gas jets and the control vanes are located at the tips of the solar panels to maximize lever arm length, in accordance with

design goal(1). Each gas jet control-actuator assembly, represented schematically in Fig. 7, is a self-contained unit requiring only a dc power source, a gas supply line, and gas jet command signals to operate. The gas jets on opposing panels operate as force couples, while the solar pressure vanes operate differentially about a preset erected position. The innermost, or torque-balancing actuation of the vanes is driven by a stepping motor and a gear train with integral electronics. The control logic is arranged so that each gas jet actuation commands one step of the vane actuator, thus increasing solar pressure torque in the same direction as that of the particular gas jet impulse. Any torque bias, resulting in a preponderance of jet pulses in a single direction to combat it, will thus cause the solar vanes to move so as to reduce the bias. The end result of such a procedure is a balanced configuration, with the solar pressure null point within the jet system dead band. Power for this adaptive balancing system is derived from the primary control system supply, through suitable isolation, with the stepping-pulse energy stored in capacitors in the vane-control electronics. Control signals are taken from the adjacent gas valves through isolation. The primary system is thus made almost completely invulnerable to any solar pressure system failure. Limit switches for vane travel are provided to minimize torque imbalance resulting from a runaway failure mode in the vane system.
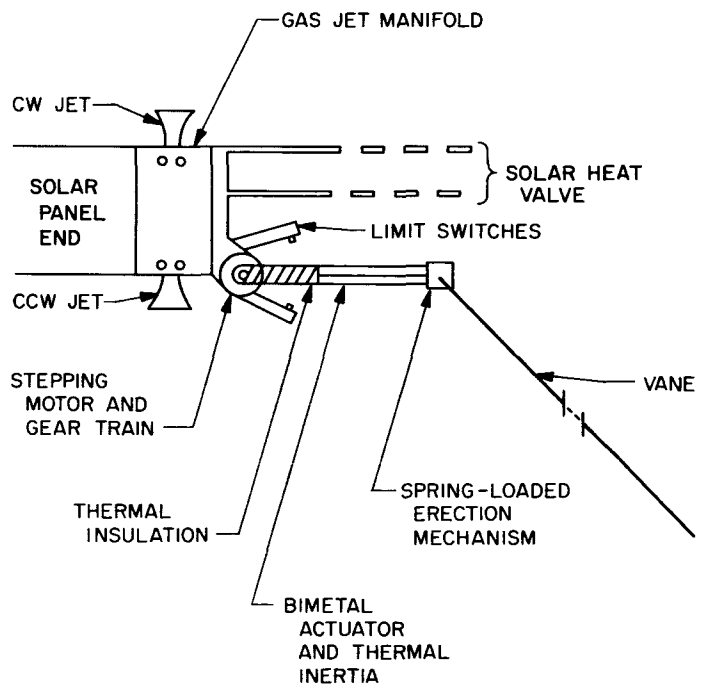

Fig. 7. Mechanization of gas jet control-actuator assembly

As the spacecraft approaches a balanced condition, characterized by less frequent jet pulses and greater penetration of the dead band, as shown in the phase plane plots of Fig. 8, the thermal–mechanical damping actuator begins to be effective. This is a phase-lagged positive position-feedback system, as described above, and is mechanized by a spacecraft-position-sensitive solar energy valve controlling the heat input to a bimetal strip with large thermal inertia. Again referring to Fig. 8, one observes that the end result will be a zero-velocity condition at a stable point somewhere within the jet dead band. Unless disturbed, the jets will not be required to operate; but, since they have not been turned off, they are ready for instant action in case of disturbance.

B. System Analysis

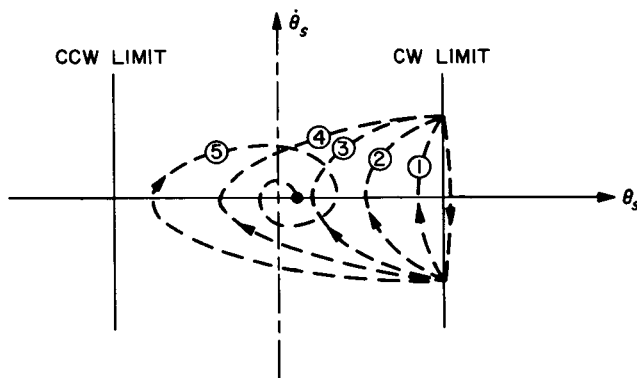A method of choosing the system parameters can be illustrated with the aid of the schematic in Fig. 9. Here,

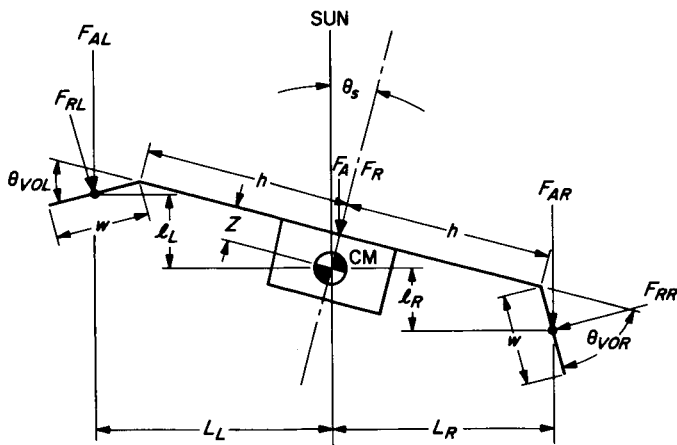**Fig. 8. Typical solar pressure control system acquisition**

Fig. 9. Schematic of statically unstable spacecraft

the center of pressure of the spacecraft without the vanes attached lies between the center of mass and the Sun. As discussed above, this is a statically unstable system. Thus, the purpose of attaching vanes is threefold: (1) to make the spacecraft system statically stable; (2) to align the stable position of the spacecraft with the null of the primary attitude control system; and (3) to supply retarding forces to damp out any oscillations that may occur.

In order to establish the vane area and the desired vane dynamics, it is necessary to determine the torque gains of the system. The term *torque gain* is used here to mean the magnitude of the value of the ratio of applied torque to the spacecraft angular position θ_s. Among the several gains to be considered, the first is that of the spacecraft without any vanes attached, denoted by K_d. Thus, for small values of θ_s,

$$T_d = K_d \theta_s \tag{8}$$

where (in this example) T_d is a destabilizing torque. The value for K_d is dependent upon the force F_a due to the absorbed radiation and, for a symmetric spacecraft, is found from the expression

$$K_d = F_a Z \tag{9}$$

Here, Z is the distance between the center of pressure of the spacecraft without vanes and its center of mass. If, for the moment, the vanes are assumed to be rigidly attached to the spacecraft, a restoring torque T_s, caused by the vanes, occurs when the spacecraft moves away from the null position. Thus,

$$T_s = -K_s \theta_s \tag{10}$$

where K_s is the stabilizing gain.

As discussed above, in order to damp out any oscillation, it is necessary to move the vanes in such a manner that the vane torques lag the spacecraft position. From some nominal or zero position, the vanes can be moved to generate this retarding torque. Letting the position gain of the vanes be K_v, the change in vane position $\Delta\theta_v$ is

$$\Delta\theta_v = \frac{-K_v}{\tau_v S + 1}\theta_s \tag{11}$$

where τ_v is the vane time constant. The torque of the vanes is described by

$$T_v = -K_T \Delta\theta_v \tag{12}$$

where K_T is the torque gain of the vanes.

The block diagram for this system (based on the assumption that the Sun is inertially fixed) is shown in Fig. 10. In the part representing the spacecraft dynamics, J is the spacecraft moment of inertia about its center of mass. Because of the inability to align the center of mass exactly with the geometric center, and because of variations in reflectivity over the exposed surface, the stable position of the spacecraft may not be the desired orientation with respect to the Sun. However, in this example, it is assumed that any bias torques have been cancelled in the manner mentioned above. (The effects of these bias torques on K_T are discussed in a subsequent paragraph of this Section.) The reference position θ_R is nominally zero.

The values of the system constants are chosen by considering the closed-loop expression for θ_s/θ_R:

$$\frac{\theta_s}{\theta_R} = \frac{K_v K_T}{(\tau_v S + 1)(JS^2 - K_d + K_s) - K_v K_T}$$

Letting

$$\omega_n = \left(\frac{K_s - K_d}{J}\right)^{1/2}$$

$$K_1 = \frac{1}{\tau_v \omega_n}$$

$$K_2 = \frac{K_v K_T}{K_s - K_d}$$

the above expression becomes

$$\frac{\theta_s}{\theta_R} = \frac{K_1 K_2 \omega_n^3}{S^3 + K_1 \omega_n S^2 + \omega_n^2 S + K_1 \omega_n^3 (1 - K_2)} \quad (13)$$

The roots of the characteristic equation can be found for various values of K_1 and K_2, and the plot shown in Fig. 11 can be constructed. Since it develops that the roots are a complex pair and a real root, both the percentage overshoot O and the damping ratio ξ are important. By means of Fig. 11, the selection of the desired values for ξ and O establishes values for K_1 and K_2.

The task that remains is to interpret the values of the physical and system constants from the desired values of K_1 and K_2. This is accomplished by considering the expressions for the torques acting on the system. Denoting the absorbed and reflected forces on the left and right vanes by F_{AL}, F_{RL}, F_{AR}, and F_{RR}, respectively, letting the area of each vane be A, assuming that the vanes are specularly reflective (i.e., $s = 1$), and referring to Fig. 9, the forces may be stated as follows:

$$F_{AL} = P_f A (1 - \rho) \cos (\theta_{VOL} - \theta_s)$$

$$F_{RL} = 2P_f A \rho \cos^2 (\theta_{VOL} - \theta_s)$$

$$F_{AR} = P_f A (1 - \rho) \cos (\theta_{VOR} + \theta_s)$$

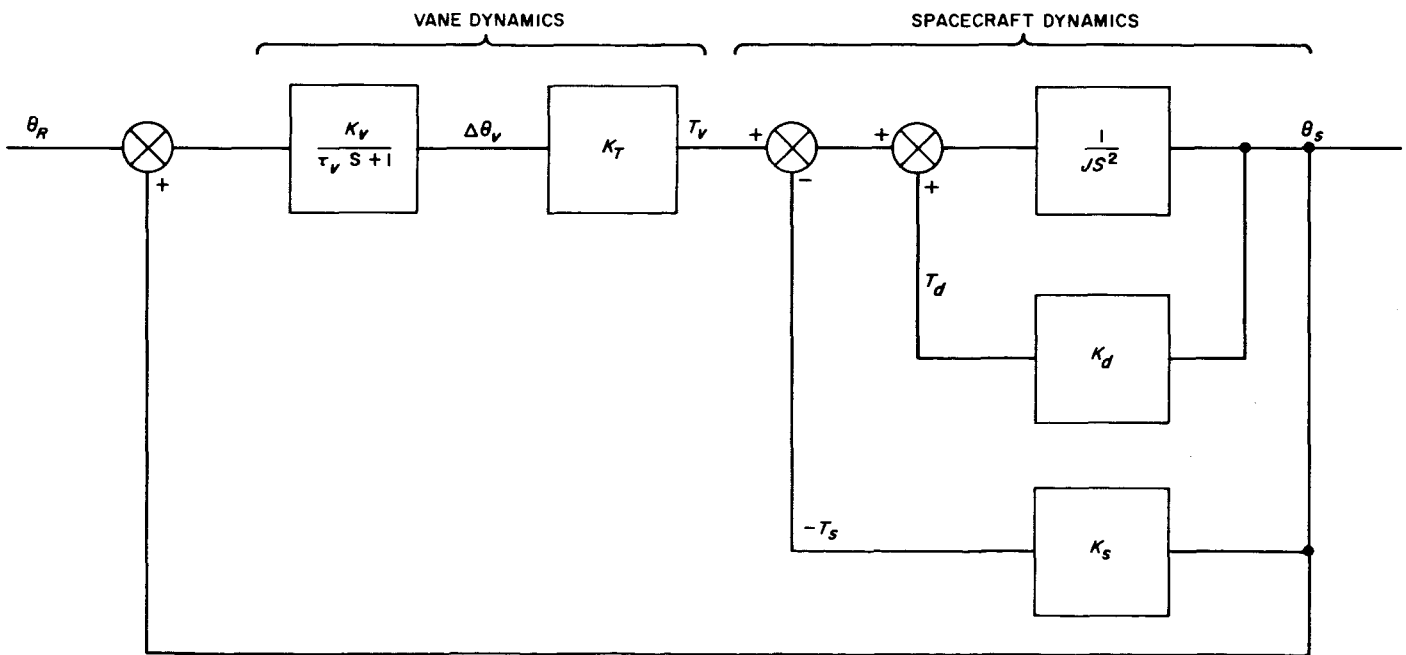$$F_{RR} = 2P_f A \rho \cos^2 (\theta_{VOR} + \theta_s)$$

Fig. 10. Block diagram of solar pressure control system for fixed Sun direction

Here, θ_{VOL} and θ_{VOR} are the respective angles formed by the left and right vanes with the solar panels. The torque T_v due to the vanes is, then,

$$T_v = \ell_L F_{RL} \sin (\theta_{VOL} - \theta_s) + \ell_R F_{RR} \sin (\theta_{VOR} + \theta_s)$$

$$- L_R \left[F_{AR} + F_{RR} \cos (\theta_{VOR} + \theta_s) \right]$$

$$- L_L \left[F_{AL} + F_{RL} \cos (\theta_{VOL} - \theta_s) \right] \tag{14}$$

where

$$\theta_{VOR} = \theta_{VO} + \Delta\theta_v$$

$$\theta_{VOL} = \theta_{VO} - \Delta\theta_v$$

and

$$\delta = \Delta\theta_v + \theta_s$$

The meaning of the quantities ℓ_L, ℓ_R, L_L, and L_R is best described by Fig. 9.

Performing the indicated substitutions and putting all variables in terms of the system parameters gives an expression for a torque-to-area ratio:

$$\frac{T_v}{A} = 2P_{f\rho} \left\{ h\theta_s \left[\cos^2 (\theta_{VO} + \delta) \sin (\theta_{VO} + \delta) \right. \right.$$

$$\left. + \cos^2 (\theta_{VO} - \delta) \sin (\theta_{VO} - \delta) \right]$$

$$+ Z \theta_s \left[\cos^3 (\theta_{VO} + \delta) + \cos^3 (\theta_{VO} - \delta) \right]$$

$$+ Z \left[\cos^2 (\theta_{VO} - \delta) \sin (\theta_{VO} - \delta) \right.$$

$$\left. - \cos^2 (\theta_{VO} + \delta) \sin (\theta_{VO} + \delta) \right]$$

$$+ h \left[\cos^3 (\theta_{VO} + \delta) - \cos^3 (\theta_{VO} - \delta) \right]$$

$$+ \frac{w}{2} \left[\cos^2 (\theta_{VO} + \delta) \sin^2 (\theta_{VO} + \delta) \right.$$

$$- \cos^2 (\theta_{VO} - \delta) \sin^2 (\theta_{VO} - \delta)$$

$$\left. + \cos^4 (\theta_{VO} + \delta) - \cos^4 (\theta_{VO} - \delta) \right] \right\}$$

$$+ P_f (1 - \rho) \left\{ Z \theta_s \left[\cos (\theta_{VO} + \delta) + \cos (\theta_{VO} - \delta) \right] \right.$$

$$+ h \left[\cos (\theta_{VO} + \delta) - \cos (\theta_{VO} - \delta) \right]$$

$$\left. + \frac{w}{2} \left[\cos^2 (\theta_{VO} + \delta) - \cos^2 (\theta_{VO} - \delta) \right] \right\} \tag{15}$$

In this expression, the vane width w may or may not be dependent on the value of A. In the discussion that fol-
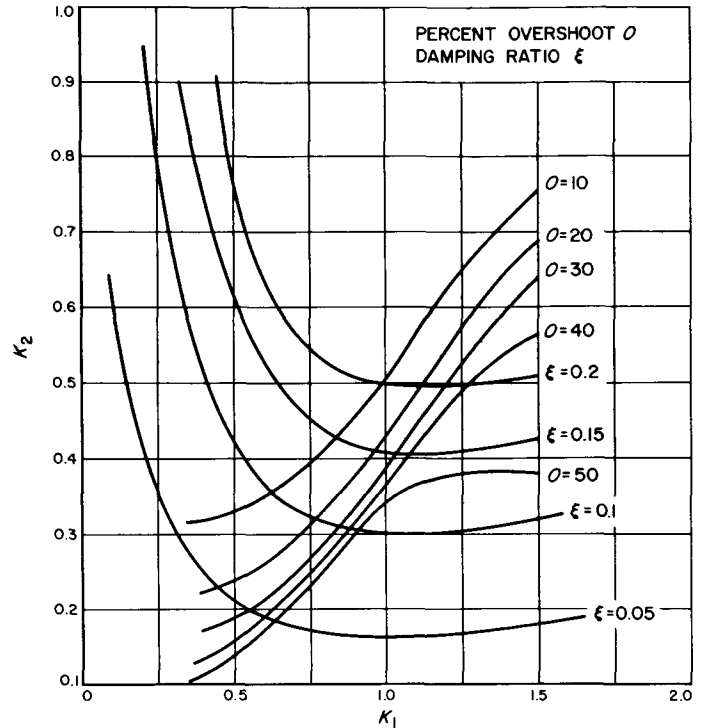

Fig. 11. Design chart for selection of K_1 and K_2

lows, it is assumed that w is independent of the vane area. However, if this is not the case, the results can be modified by finding the expression for

$$\frac{\partial \dfrac{T_v}{A}}{\partial w}$$

and using its value to calculate an appropriate correction factor. The validity of the new results obtained will depend upon the accuracy of the original estimate of w and the magnitude of the partial derivative. The value for θ_{VO} is determined by assuming $\theta_s = 0$ and finding the value for θ_{VO} which maximizes the expression

$$\frac{\partial \dfrac{T_v}{A}}{\partial \delta} = - \frac{K_T}{A} \tag{16}$$

A curve of T_v/A as a function of δ can then be plotted. In this example,

$$P_f = 0.47 \text{ dynes/m}^2$$

$$\rho = 0.8$$

$$h = 224 \text{ cm}$$

$Z = 30.5 \, \text{cm}$

$w = 61 \, \text{cm}$

For these values, $\theta_{VO} = 37.5$ deg. The resulting curve for T_v/A, shown in Fig. 12, has a slope of $- K_T/A$.

If bias torques are initially acting on the spacecraft, the steady state position of the vanes will be at some angle $\Delta\theta_v$ away from θ_{VO}. Since the gain, expressed by

$$-\frac{K_s}{A} = \frac{\partial \dfrac{T_v}{A}}{\partial \theta_s}$$

is dependent upon $\Delta\theta_v$, it is necessary to determine K_s/A as a function of $\Delta\theta_v$. The results of this computation are shown in Fig. 13.

Sufficient information is now available to determine the values of the physical and system constants. The approach can best be explained by using the curves obtained in the example above. Assume that a minimum damping ratio of 0.15 and a maximum overshoot of 30% are desired. Then, from Fig. 11,

$$K_1 = 1.03$$

$$K_2 = 0.41$$

Assume also that the maximum expected bias torque is 75 dyne-cm, and that the destabilizing gain K_d at the spacecraft is 2.5 dyne-cm/deg. It must now be decided what degradation in gain K_s will be acceptable as the vanes move to cancel the bias torque. Assume this to be 10%. Then, from Fig. 13, a 10% degradation of K_s allows a $\Delta\theta_v$ of 11 deg, and

$$6.0 \times 10^{-4} \frac{\text{dyne-cm}}{\text{cm}^2\text{-deg}} \leq \frac{K_s}{A} \leq 6.67 \times 10^{-4} \frac{\text{dyne-cm}}{\text{cm}^2\text{-deg}}$$

Using Fig. 12, considering a maximum bias torque of 75 dyne-cm, and taking $(\Delta\theta_v)_{max} = 11$ deg, one obtains, for the area A of each vane,

$$A = 7500 \, \text{cm}^2$$

This is approximately 8 ft² and represents the minimum area that can be used. The range of values for K_s is, then,

$$4.5 \frac{\text{dyne-cm}}{\text{deg}} \leq K_s \leq 5.0 \frac{\text{dyne-cm}}{\text{deg}}$$
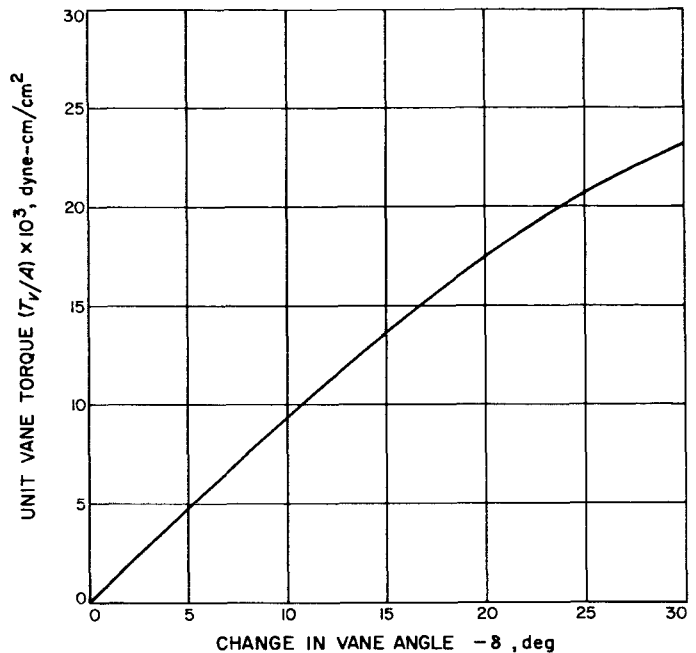

Fig. 12. Graph for determination of vane torque gain
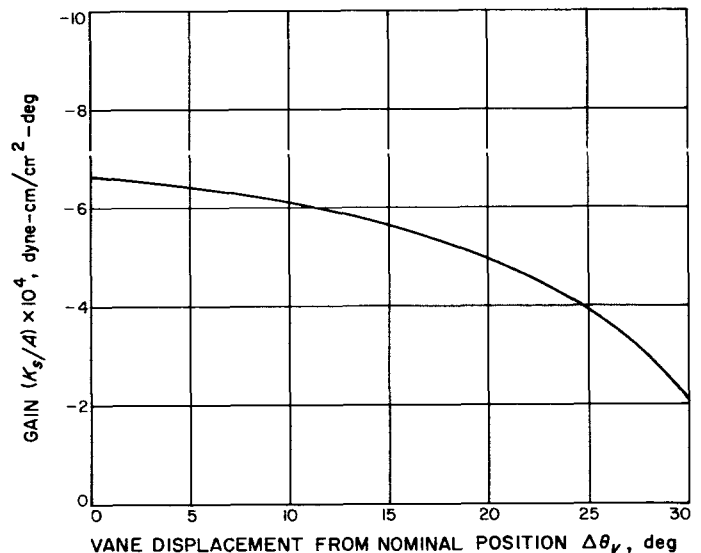

Fig. 13. Stabilizing gain of vanes as a function of vane angle

Assume that

$$K_s = 4.75 \frac{\text{dyne-cm}}{\text{deg}}$$

Then, for $J = 8.13 \times 10^8$ dyne-cm-sec²,

$$\tau_v = 2430 \, \text{sec}$$

From Fig. 14, with $A = 7500$ cm^2, the value of K_T has the range

$$6.68 \frac{\text{dyne-cm}}{\text{deg}} \leq K_T \leq 7.2 \frac{\text{dyne-cm}}{\text{deg}}$$

for $0 \leq \Delta\theta_v \leq 11$ deg. Using

$$K_T = 6.9 \frac{\text{dyne-cm}}{\text{deg}}$$

then

$$K_v = 0.134 \frac{\text{degrees of vane motion}}{\text{degrees of spacecraft motion}}$$

Thus, the system parameters and physical constants have been established.

The preceding analysis is based on the assumption that the Sun is fixed in inertial space. If this assumption is dropped, the block diagram of the system is as shown in Fig. 15. In this diagram, θ_R is the angle between an inertial reference direction and the Sun direction. The variable ϕ is the angle between the same inertial reference and the spacecraft pointing direction. As before, θ_s is the rotation of the spacecraft with respect to the Sun line. The transfer function of interest is now

$$\frac{\phi}{\theta_R} = \frac{\omega_n^2 \left[S + K_1\omega_n (1 - K_2) \right]}{S^3 + K_1\omega_n S^2 + \omega_n^2 S + K_1\omega_n^3 (1 - K_2)} \qquad (17)$$

Note that the characteristic equation is the same as Eq. 13; thus, the change of parameters is valid. Since Eq. 17 has unity gain for steady state, it indicates that, as the spacecraft moves around the Sun, the nominal spacecraft angle θ_s will remain zero.
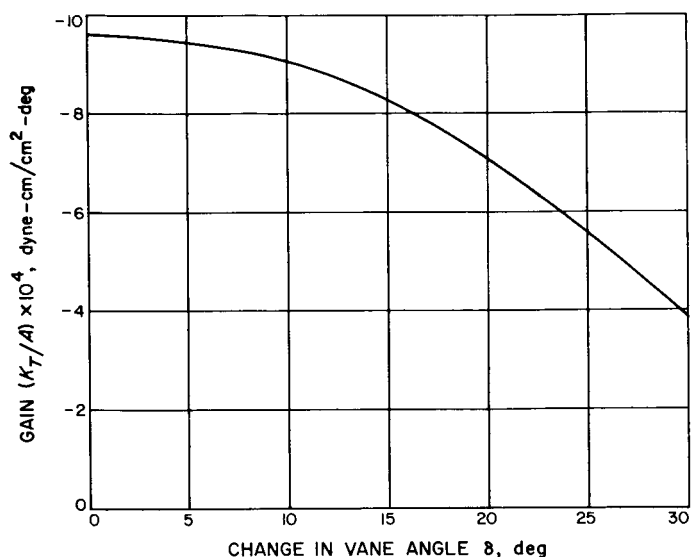

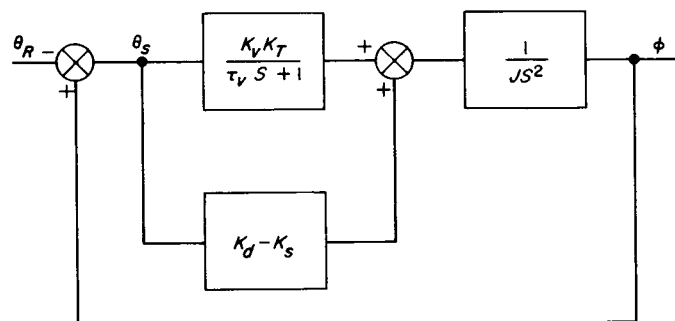Fig. 14. Torque gain of vanes vs change in vane angle

Fig. 15. Block diagram of solar pressure control system for varying Sun direction

IV. SPECIAL MECHANIZATION CONSIDERATIONS

The block diagram in Fig. 10 and the derived transfer function give no hint that the system is other than a normal homing-type position servo system. A few calculations based on a representative system design will, however, illustrate some of the special mechanization problems.

Consider a design based on the following parameters, as mentioned in the foregoing analysis:

Spacecraft moment of inertia:

$$J = 8.13 \times 10^8 \text{ dyne-cm-sec}^2$$

Vane area (each vane):

$$A = 7.5 \times 10^3 \text{ cm}^2$$

Spacecraft restoring-force constant:

$$(K_s - K_d) = 2.25 \text{ dyne-cm/deg}$$
$$= 130 \text{ dyne-cm/rad}$$

The undamped natural frequency of oscillation ω_n is, then,

$$\omega_n = \left(\frac{K_s - K_d}{J}\right)^{\frac{1}{2}} = \left(\frac{1.3 \times 10^2}{8.13 \times 10^8}\right)^{\frac{1}{2}}$$

$$= 4 \times 10^{-4}\,\text{rad/sec}$$

or, on a more comprehensible scale, $f_n = 0.23$ cycles/hr.

Any type of control-loop compensation, either lead or lag, real or complex, must yield significant phase shift at this frequency to be effective. In the system described, a time constant of 2430 sec was chosen as the best balance between a number of competing considerations. Actually, in establishing tolerances, a longer time constant is less degrading to system performance than a shorter one. The specific problem in the example chosen is to mechanize, for spacecraft angular excursions θ_s of a few degrees, a control-vane motion rising exponentially toward a final value of 0.134 θ_s, with a time constant of 2430 sec.

A very complex system would result if this transfer function were to be mechanized using conventional electro-mechanical techniques. The block diagram in Fig. 16 illustrates the functional elements involved. The resulting transfer function is

$$\frac{\Delta\theta_v}{\theta_s} = \frac{KK'}{1 + 2430S}$$

which meets the specified requirements if $KK' = 0.134$. The complication results because:

1. In an electromagnetic radiation energy system, the basic information (the direction of the Sun) is first converted to an electrical signal, then processed electronically, and finally converted to a mechanical output (the vane motion).

2. Electronic information processing is awkward on the slow time scales involved because of electronic-component limitations.
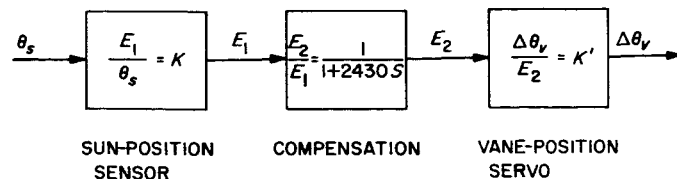
In contrast, if the electromagnetic radiation energy system is used directly until the final conversion to a mechanical output, several advantages are apparent:

1. No electrical power is required for operation.

2. A much simpler configuration, with fewer and less complex components, results.

3. The time scales involved are ideal for thermal-mechanical components of reasonable size and weight.

Figure 17 presents a schematic diagram illustrating the simplicity of mechanization for this system. The bimetal strip acts as both compensation network and vane position servo, while the shadow-bar arrangement acts as position sensor and error amplifier. In operation, if the system is assumed to be in an equilibrium position defined by

$$Q_{out} = Q_0,\ T = T_0,\ \theta_s = 0,\ \Delta\theta_v = 0$$

and θ_s is given a value at $t = 0$, the bimetal-strip temperature will proceed toward a new equilibrium in an approximately exponential fashion. The time constant will be determined by thermal inertia in the bimetal strip, by heat leakage, and, because of the nonlinear character of the reradiation function, by the initial equilibrium temperature. The latter effect is small, however, resulting in only a small change in damping ratio (about 15%) for a 50% change in solar constant. The steady-state angle-to-angle gain from θ_s to $\Delta\theta_v$ is determined primarily by the shadow-bar lever arm.

It must be emphasized that the damping-loop mechanization described is not passive as is the restoring-torque mechanization. It merely avoids the use of an electrical energy system.
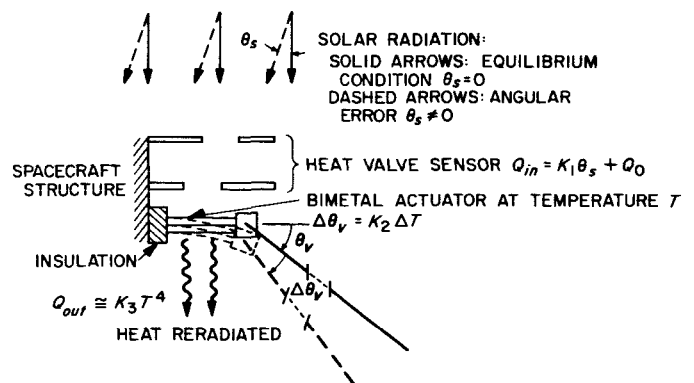

Fig. 16. Block diagram of thermal–mechanical control actuator

Fig. 17. Operational diagram of thermal–mechanical actuator

V. CONCLUSION

A practical attitude control system utilizing forces generated by solar pressure is described in this Report. The system has several advantages over other systems discussed in the literature. The question of obtaining suitable damping has been considered, and a technique of achieving it is given. The design procedure can be organized in such a manner that the system parameters or the effects of changes in the parameters can be quickly determined. The mechanization is such that all components are state of the art and can be ground-tested. Solar pressure control is integrated into the primary attitude control system in a manner that permits mission success if a failure occurs in any of the solar pressure control components. Finally, inclusion of solar pressure control increases mass efficiency, as well as system reliability as a whole.

REFERENCES

1. Hall, H. B., The Effect of Radiation Force on Satellites of Convex Shape, Technical Note D-604, National Aeronautics and Space Administration, Washington, D.C., May 1961.

2. Kozai, Y., "Effects of Solar Radiation Pressure on the Motion of an Artificial Satellite," Research in Space Science, Special Report 56, pp. 25–33, Smithsonian Institution, Astrophysical Observatory, Cambridge, Mass., January 30, 1961.

3. Ives, N. E., The Effect of Solar Radiation Pressure on the Attitude Control of an Artificial Earth Satellite, Technical Note G.W. 570, Royal Aircraft Establishment, Farnborough, Great Britain, April 1961.

4. Sohn, R. L., "Attitude Stabilization by Means of Solar Radiation Pressure," ARS Journal, Vol. 29, No. 5, pp. 371–373, May 1959.

5. Frye, W. E., and Sterns, E. V. B., "Stabilization and Attitude Control of Satellite Vehicles," ARS Journal, Vol. 29, No. 12, pp. 927–931, December 1959.

6. Newton, R. R., "Stabilizing a Spherical Satellite by Radiation Pressure," ARS Journal, Vol. 30, No. 12, pp. 1175–1176, December 1960.

7. Nicklas, J. C., and Vivian, H. C., "Derived-Rate Increment Stabilization: Its Application to the Attitude Control Problem," ASME Transactions, Series D—Journal of Basic Engineering, Vol. 84, No. 1, pp. 54–60, March 1962.